Soil Moisture Active Passive (SMAP)

Algorithm Theoretical Basis Document (ATBD)

SMAP Level 3 Radiometer Freeze/Thaw Data Products (L3_FT_P and L3_FT_P_E)

Revision A
October 15, 2016

Scott Dunbar, Xiaolan Xu, Andreas Colliander
Jet Propulsion Laboratory
California Institute of Technology
Pasadena, CA

Chris Derksen
Climate Research Division, Environment Canada
Toronto, Canada

John Kimball and Youngwook Kim
University of Montana
Missoula, MT

JPL D-56288

(Page intentionally left blank)

The SMAP Algorithm Theoretical Basis Documents (ATBDs) provide the physical and mathematical descriptions of the algorithms used in the generation of science data products. The ATBDs include a description of variance and uncertainty estimates and considerations of calibration and validation, exception control and diagnostics. Internal and external data flows are also described.

Table of Contents

ACRONYMS AND ABBREVIATIONS

AMSR	Advanced Microwave Scanning Radiometer
ASF	Alaska Satellite Facility
ATBD	Algorithm Theoretical Basis Document
CONUS	Continental United States
CMIS	Conical-scanning Microwave Imager Sounder
DAAC	Distributed Active Archive Center
DCA	Dual Channel Algorithm
DEM	Digital Elevation Model
EASE	Equal Area Scalable Earth [grid]
ECMWF	European Center for Medium-Range Weather Forecasting
EOS	Earth Observing System
ESA	European Space Agency
GEOS	Goddard Earth Observing System (model)
GMAO	Goddard Modeling and Assimilation Office
GSFC	Goddard Space Flight Center
JAXA	Japan Aerospace Exploration Agency
JPL	Jet Propulsion Laboratory
LTAN	Local Time of Ascending Node
LTDN	Local Time of Descending Node
MODIS	MODerate-resolution Imaging Spectroradiometer
NCEP	National Centers for Environmental Prediction
NDVI	Normalized Difference Vegetation Index
NEE	Net ecosystem exchange
NPOESS	National Polar-Orbiting Environmental Satellite System
NPP	NPOESS Preparatory Project
NSIDC	National Snow and Ice Data Center
NWP	Numerical Weather Prediction
OSSE	Observing System Simulation Experiment
PDF	Probability Density Function
PGE	Product Generation Executable
RFI	Radio Frequency Interference
RVI	Radar Vegetation Index
SAR	Synthetic Aperture Radar
SDT	(SMAP) Science Definition Team
SDS	(SMAP) Science Data System
SMAP	Soil Moisture Active Passive
SMOS	Soil Moisture Ocean Salinity (mission)
SNR	Signal to Noise Ratio
SRTM	Shuttle Radar Topography Mission
USGS	United States Geological Survey
VWC	Vegetation Water Content

1 INTRODUCTION

The Level 3 radiometer landscape freeze/thaw product (L3_FT_P) provides a daily classification of freeze/thaw state for land areas north of 45°N derived from the SMAP radiometer, output to 36 km northern polar and global EASE grid formats. The same freeze/thaw retrieval algorithm can be applied to optimally interpolated SMAP radiometer brightness temperature retrievals to produce the enhanced resolution freeze/thaw product (L3_FT_P_E) posted at 9 km grid spacing. This document provides a complete description of the algorithm used to generate the L3_FT_P and L3_FT_P_E products, including the physical basis, theoretical description, and practical considerations for implementing the algorithm, and the validation approach for determining performance against the mission requirement. ***The algorithm and processing are identical for both FT_P products – the only difference is the spatial resolution of the brightness temperature inputs. Unless specifically noted otherwise, references to L3_FT_P also cover L3_FT_P_E because the same algorithm and processing chain apply to both products.***

1.1 THE SOIL MOISTURE ACTIVE PASSIVE (SMAP) MISSION

1.1.1 BACKGROUND AND SCIENCE OBJECTIVES

The National Research Council's (NRC) Decadal Survey, *Earth Science and Applications from Space: National Imperatives for the Next Decade and Beyond*, was released in 2007 after a two year study commissioned by NASA, NOAA, and USGS to provide them with prioritization recommendations for space-based Earth observation programs [National Research Council, 2007]. Factors including scientific value, societal benefit and technical maturity of mission concepts were considered as criteria. SMAP data products have high science value and provide data towards improving many natural hazards applications. Furthermore SMAP draws on the significant design and risk-reduction heritage of the Hydrosphere State (Hydros) mission [Entekhabi et al., 2004]. For these reasons, the NRC report placed SMAP in the first tier of missions in its survey. In 2008 NASA announced the formation of the SMAP project as a joint effort of NASA's Jet Propulsion Laboratory (JPL) and Goddard Space Flight Center (GSFC), with project management responsibilities at JPL. The observatory was launched in January 2015.

As described in Entekhabi et al. [2010], the SMAP science and applications objectives are to:

- Understand processes that link the terrestrial water, energy and carbon cycles;
- Estimate global water and energy fluxes at the land surface;
- Quantify net carbon flux in boreal landscapes;
- Enhance weather and climate forecast skill;
- Develop improved flood prediction and drought monitoring capabilities.

1.1.2 MEASUREMENT APPROACH

Table 1 is a summary of the SMAP instrument functional requirements derived from its science measurement needs. The original goal was to combine the attributes of the radar and

radiometer observations (in terms of their spatial resolution and sensitivity to soil moisture, surface roughness, and vegetation) to estimate soil moisture at a resolution of 10 km, and freeze/thaw state at a resolution of 3 km.

Table 1. SMAP mission requirements.

Scientific Measurement Requirements	Instrument Functional Requirements
Soil Moisture: ~±0.04 m^3m^{-3} volumetric accuracy(1-sigma) in the top 5 cm for vegetation water content ≤ 5 kg m^{-2}; Hydrometeorology at ~10 km resolution; Hydroclimatology at ~40 km resolution	L-Band Radiometer (1.41 GHz): Polarization: V, H, T_3 and T_4 Resolution: 40 km Radiometric Uncertainty*: 1.3 K L-Band Radar (1.26 and 1.29 GHz): Polarization: VV, HH, HV (or VH) Resolution: 10 km Relative accuracy*: 0.5 dB (VV and HH) Constant incidence angle** between 35° and 50°
Freeze/Thaw State: Capture freeze/thaw state transitions in integrated vegetation-soil continuum with two-day precision, at the spatial scale of landscape variability (~3 km)	L-Band Radiometer (1.41 GHz): Polarization: V, H, T_3 and T_4 Resolution: 40 km Radiometric Uncertainty*: 1.3 K Constant incidence angle** between 35° and 50°
Sample diurnal cycle at consistent time of day (6am/6pm Equator crossing); Global, ~3 day (or better) revisit; Boreal, ~2 day (or better) revisit	Swath Width: ~1000 km Minimize Faraday rotation (degradation factor at L-band)
Observation over minimum of three annual cycles	Baseline three-year mission life
* Includes precision and calibration stability ** Defined without regard to local topographic variation	

The SMAP spacecraft is designed for a 685-km circular, sun-synchronous orbit, with equator crossings at 6 AM and 6 PM local time. The instrument combines radar and radiometer subsystems that share a single feedhorn and parabolic mesh reflector (Fig. 1). The radar operates with VV, HH, and HV transmit-receive polarizations, and uses separate transmit frequencies for the H (1.26 GHz) and V (1.29 GHz) polarizations. The radiometer operates with polarizations V, H, and the third and fourth Stokes parameters, T_3, and T_4, at 1.41 GHz. The T_3-channel measurement is used to assist in the correction of Faraday rotation effects. The reflector is offset from nadir and rotates about the nadir axis at 14.6 rpm, providing a conically scanning antenna beam at a surface incidence angle of approximately 40°. The provision of constant incidence angle across the swath simplifies the data processing and enables accurate repeat-pass estimation of soil moisture and freeze/thaw change. The reflector diameter is 6 m, providing a radiometer footprint of approximately 40 km (root-ellipsoidal area) defined by the one-way 3-dB beamwidth. The two-way 3-dB beamwidth defines the real-aperture radar footprint of approximately 30 km. The real-aperture ('lo-res') swath width of 1000 km provides global coverage within 3 days or less equatorward of 35°N/S and 2 days poleward of 55°N/S. The real-aperture radar and radiometer data will be collected globally during both ascending and descending passes.

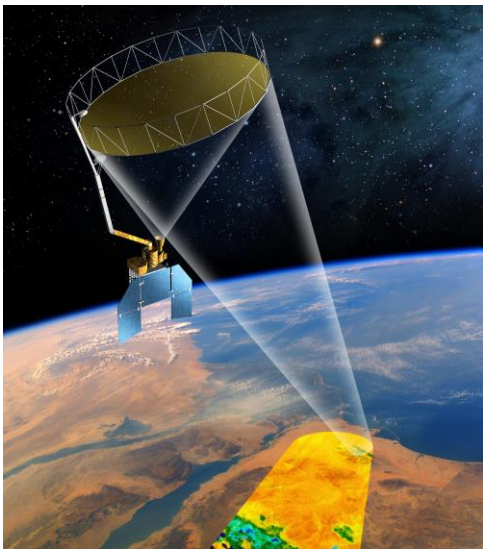

Figure 1. The SMAP observatory is a dedicated spacecraft with a rotating 6-m light-weight deployable mesh reflector. The radar and radiometer share a common feed.

The baseline orbit parameters are:

- Orbit Altitude: 685 km (2-3 days average revisit and 8-days exact repeat)
- Inclination: 98 degrees, sun-synchronous
- Local Time of Ascending Node: 6 pm

At L-band anthropogenic Radio Frequency Interference (RFI), principally from ground-based surveillance radars, can contaminate both radar and radiometer measurements. Early measurements and results from the SMOS mission indicate that in some regions RFI is present and detectable. The SMAP radar and radiometer electronics and algorithms have been designed to include features to mitigate the effects of RFI. To combat this, the SMAP radar utilizes selective filters and an adjustable carrier frequency in order to tune to pre-determined RFI-free portions of the spectrum while on orbit. The SMAP radiometer will implement a combination of time and frequency diversity, kurtosis detection, and use of T_4 thresholds to detect and where possible mitigate RFI.

The SMAP L1-L4 data products are listed in Table 2. Level 1B and 1C data products are calibrated and geolocated instrument measurements of surface radar backscatter cross-section and brightness temperatures derived from antenna temperatures. Level 2 products are geophysical retrievals of soil moisture on a fixed Earth grid based on Level 1 products and ancillary information; the Level 2 products are output on half-orbit basis. Level 3 products are daily composites of Level 2 surface soil moisture and freeze/thaw state data. Level 4 products are model-derived value-added data products that support key SMAP applications and more directly address the driving science questions.

Table 2. SMAP data products.

Product	Description	Gridding (Resolution)	Latency**	
L1A_Radiometer	Radiometer Data in Time-Order	-	12 hrs	Instrument Data
L1A_Radar	Radar Data in Time-Order	-	12 hrs	
L1B_TB	Radiometer T_B in Time-Order	(36x47 km)	12 hrs	
L1B_TB_E	Radiometer T_B Optimally Interpolated on EASE2.0 grid	9 km	12 hrs	
L1B_S0_LoRes	Low Resolution Radar σ_o in Time-Order	(5x30 km)	12 hrs	
L1C_S0_HiRes	High Resolution Radar σ_o in Half-Orbits	1 km (1-3 km)	12 hrs	
L1C_TB	Radiometer T_B in Half-Orbits	36 km	12 hrs	
L1C_TB_E	Radiometer T_B in Half-Orbits, Enhanced	9 km	12 hrs	
L2_SM_A	Soil Moisture (Radar)	3 km	24 hrs	Science Data (Half-Orbit)
L2_SM_P	Soil Moisture (Radiometer)	36 km	24 hrs	
L2_SM_P_E	Soil Moisture (Radiometer, Enhanced))	9 km	24 hrs	
L2_SM_AP	Soil Moisture (Radar + Radiometer)	9 km	24 hrs	
L2_SM_SP	Soil Moisture (Sentinel Radar + Radiometer)	3 km	Best effort	
L3_FT_A	Freeze/Thaw State (Radar)	3 km	50 hrs	Science Data (Daily Composite)
L3_FT_P	Freeze/Thaw State (Radiometer)	36 km	50 hrs	
L3_FT_P_E	Freeze/Thaw State (Radiometer, Enhanced)	9 km	50 hrs	
L3_SM_A	Soil Moisture (Radar)	3 km	50 hrs	
L3_SM_P	Soil Moisture (Radiometer)	36 km	50 hrs	
L3_SM_P_E	Soil Moisture (Radiometer, Enhanced)	9 km	50 hrs	
L3_SM_AP	Soil Moisture (Radar + Radiometer)	9 km	50 hrs	
L4_SM	Soil Moisture (Surface and Root Zone)	9 km	7 days	Science Value-Added
L4_C	Carbon Net Ecosystem Exchange (NEE)	9 km	14 days	

1.2 SMAP Requirements Related to Freeze/Thaw State

The primary science objectives for SMAP directly relevant to the freeze/thaw product include linking terrestrial water, energy and carbon cycle processes, quantifying the net carbon flux in boreal landscapes and reducing uncertainties regarding the so-called missing carbon sink on land. This leads to the following requirements on the freeze/thaw measurement:

1) *surface freeze/thaw measurements shall be provided over land areas where these factors are primary environmental controls on land-atmosphere exchanges of water, energy and carbon;*

2) *the freeze/thaw status of the aggregate vegetation-soil layer shall be determined sufficiently to characterize the low-temperature constraint on vegetation net primary productivity and surface-atmosphere CO_2 exchange;*

3) *SMAP shall measure landscape freeze/thaw with a spatial resolution of 3 km using radar inputs, and 36 km (baseline; or best available) resolution using radiometer inputs;*

4) *SMAP shall measure landscape freeze/thaw with a mean temporal sampling of 2 days or better;*

5) *SMAP shall measure freeze/thaw with accuracy sufficient to resolve the temporal dynamics of net ecosystem exchange to within 0.05 tons C ha^{-1} (or 3%) over a ~100-day growing season.*

Current SMAP baseline mission requirements specific to terrestrial freeze/thaw science activities state that:

[Level 1 mission requirement] The original baseline science mission shall provide estimates of surface binary freeze/thaw state for the region north of 45° N latitude, which includes the boreal forest zone, with a mean spatial classification accuracy of 80% at 3 km spatial resolution and 2-day average intervals.

Given the failure of the SMAP radar in July 2015, this original mission requirement will continue to be addressed albeit at reduced spatial resolutions of 36 km and 9 km using SMAP radiometer inputs. The switch to passive inputs combined with a coarser spatial resolution will introduce fundamental differences in algorithm performance and product specifications for L3_FT_P compared to the SMAP radar derived product (L3_FT_A; April – July 2015). This document includes a description of the radiometer freeze/thaw state classification algorithm, discussion of theoretical assumptions, procedures for refining and testing the algorithm, and validation activities to assess the L3_FT_P and L3_FT_P_E products against the mission requirement.

2 BACKGROUND AND HISTORICAL PERSPECTIVE

The terrestrial cryosphere comprises cold areas of Earth's land surface where water is either permanently or seasonally frozen. This includes most regions north of 45°N latitude and most areas with elevation greater than 1000 meters. Within the terrestrial cryosphere, spatial patterns and timing of landscape freeze/thaw state transitions are highly variable with measurable impacts to climate, hydrological, ecological and biogeochemical processes.

Landscape freeze/thaw state influences the seasonal amplitude and partitioning of surface energy exchange strongly, with major consequences for atmospheric profile development and regional weather patterns (Betts et al., 2000). In seasonally frozen environments, ecosystem responses to seasonal thaw are rapid, with soil respiration and plant photosynthetic activity accelerating with warmer temperatures and the abundance of liquid water (e.g., Goulden et al.,

1998; Black et al., 2000; Jarvis and Linder, 2000). The timing of seasonal freeze/thaw transitions can generally be related to the duration of seasonal snow cover, frozen soils, and the timing of lake and river ice breakup and flooding in the spring (Kimball et al., 2001, 2004a). The seasonal non-frozen period also bounds the vegetation growing season, while annual variability in freeze/thaw timing has a direct impact on net primary production and net ecosystem CO_2 exchange (NEE) with the atmosphere (Vaganov et al., 1999; Goulden et al., 1998).

Satellite-borne microwave remote sensing has unique capabilities that allow near real-time monitoring of freeze/thaw state, without many of the limitations of optical-infrared sensors such as solar illumination or atmospheric conditions. The SMAP L3_FT_P product is designed to provide an accurate remote sensing-based characterization of landscape freeze/thaw state for land areas north of 45°N latitude. The design of the SMAP L-band radiometer allows for a combined spatial and temporal characterization of terrestrial freeze/thaw transitions that is improved compared to pre-existing L-band missions (i.e. SAC-D Aquarius – Xu et al., 2016; SMOS – Rautiainen et al., 2016). Enhanced resolution SMAP level 1 radiometer measurements will also be utilized as inputs to the freeze/thaw algorithm. Furthermore, the overlap period of SMAP radar and radiometer measurements in the spring of 2015 allows investigation of the impact of spatial resolution and differences in the strength of the freeze/thaw signal between the active and passive measurements at L-band.

The SMAP L3_FT_P baseline algorithm follows from an extensive heritage of previous work, initially involving truck mounted radar scatterometer and radiometer studies over bare soils and croplands (Ulaby et al., 1986; Wegmuller, 1990), followed by aircraft SAR campaigns over boreal landscapes (Way et al., 1990), and subsequently from a variety of satellite-based SAR, radiometer, and scatterometer studies at regional, continental and global scales (Rignot and Way, 1994; Rignot et al., 1994; Way et al., 1997; Frolking et al., 1999; Wisman, 2000; Kimball et al., 2001; 2004a,b; McDonald et al., 2004; Rawlins et al., 2005; Du et al. 2014; Podest et al. 2014; Kim et al. 2014a; Rautiainen et al., 2014; Roy et al., 2015). These investigations have included regional, pan-boreal, and global scale efforts, supporting development of retrieval algorithms, assessment of applications of remotely sensed freeze/thaw state for supporting ecologic and hydrological studies, and the assembly of a global-scale Earth System Data Record (ESDR) developed from higher frequency (37 GHz) overlapping SMMR, SSM/I and AMSR-E sensor records (Kim, et al., 2011; 2012). The global freeze/thaw ESDR is the first of its kind, providing daily freeze/thaw state across multiple decades and including delineation of AM/PM freeze/thaw transitional states.

The SMAP L3_FT_P algorithm classifies the land surface freeze/thaw state based on the time series L-band radiometer brightness temperature response to the change in dielectric constant of the land surface components associated with water transitioning between solid and liquid phases. There is a clear freeze/thaw signal in the L-band brightness temperature polarization ratio for regions of the global land surface undergoing seasonal freeze/thaw transitions (Rautiainen et al., 2012). While the lower frequency (L-band) brightness temperature measurements from SMAP provide enhanced sensitivity to freeze/thaw conditions compared to higher frequencies, uncertainties due to vegetation biomass, snow, and thick organic soil layers, do exist (Roy et al., 2015). Brightness temperature sensitivity to the freeze/thaw signal will vary

due to the underlying sub-grid heterogeneity in these landscape elements (Podest et al. 2014; Du et al. 2014).

The timing of the springtime freeze/thaw state transitions corresponding to the brightness temperature response coincides with the timing of growing season initiation in boreal, alpine and arctic tundra regions of the global cryosphere. Interannual variability in these processes is a major control on annual vegetation productivity and land-atmosphere CO_2 exchange (Frolking et al., 1999; Kimball et al., 2004; McDonald et al., 2004). Thus the L3_FT_P algorithm supports characterization of the spatial and temporal dynamics of landscape freeze/thaw state for regions of the global land surface where (1) cold temperatures are limiting for photosynthesis and respiration processes, (2) the timing and variability in landscape freeze/thaw processes have a key impact on vegetation productivity and the carbon cycle, and (3) the thermal state of the soil has a strong influence on surface hydrological processes.

2.1 PRODUCT/ALGORITHM OBJECTIVES

Figure 2 shows the data sets and processing chain associated with SMAP freeze/thaw algorithm implementation and product generation, including input and output data. The L3_FT_P product consists of daily composite landscape freeze/thaw state derived from the AM (descending) and PM (ascending) overpass radiometer data (L1C_TB half-orbits) north of 45°N. The L3_FT_P product is gridded and provided on a 36 km Equal Area Scalable Earth grid version 2 (EASE-grid) in both global and north polar projections. The same data flow applies to the enhanced resolution product (L3_FT_P_E) with L1C_TB at 36 km replaced by L1C_TB_E at 9 km resolution.

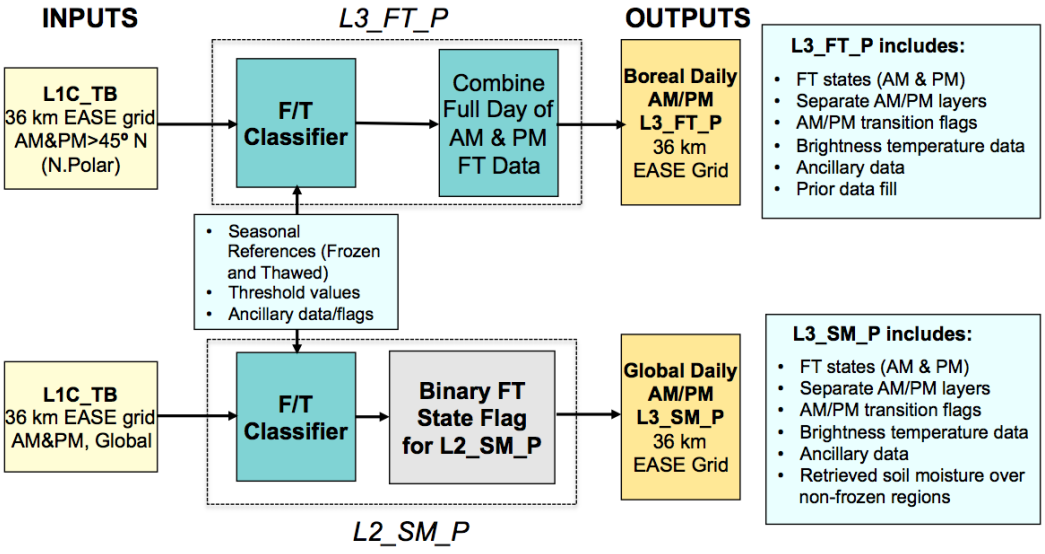

Figure 2. Processing sequence for generation of the L3_FT_P product and the binary freeze/thaw state flag for use in L2_SM_P.

The baseline L3_FT_P product provides freeze/thaw state classification information at a spatial resolution of 36 km with temporal revisit of 2 days or better north of ~55°N and 3 days or better north of 45°N. The freeze/thaw classification domain covers regions of Earth's land mass where low temperatures are a significant constraint to vegetation productivity and terrestrial carbon exchange (Churkina and Running, 2000; Nemani et al., 2003; Kim et al., 2011). Product accuracy associated with meeting SMAP mission requirements is focused solely on the freeze/thaw domain north of 45°N latitude.

Freeze/thaw state is generated separately for AM and PM radiometer acquisitions. Combining SMAP freeze/thaw state assessments from AM and PM acquisitions for the L3_FT_P product (upper processing chain in Figure 2) provides information on regions undergoing freeze/thaw transitions on a diurnal basis (e.g. Kim et al., 2011). This aspect of the product supports enhanced investigation of spring and autumn transition seasons and the associated controls on annual vegetation productivity (e.g. Kim et al. 2012).

The radiometer freeze/thaw algorithm is also integrated into the L2_SM_P processor to supply a 36 km resolution global binary freeze/thaw state flag that is utilized by the L2_SM_P radiometer soil moisture processing to identify frozen land regions, supporting the generation of the L2 and L3 passive soil moisture products (L2/3_SM_P; lower processing chain in Figure 2). Accuracy of the AM and PM overpass freeze/thaw estimates for regions south of 45°N, which will feed into other SMAP products, will be assessed as part of SMAP L4 product cal/val activities.

The 45°N latitude limit for the L3_FT_P product was established because freeze/thaw transitions, particularly in non-alpine regions, tend to be ephemeral below approximately 45°N. As shown in Figure 3, there is widespread positive correspondence between variability in the length of the non-frozen season (derived from SSM/I 37 GHz brightness temperatures) and NDVI summer growth changes (derived from the MODIS MOD13 NDVI record) over northern (>=45°N) land areas, consistent with frozen season constraints on vegetation productivity over the northern domain (Kim et al., 2012). The relative influence of freeze/thaw and non-frozen season effects on vegetation growth is less widespread at lower latitudes due to a general reduction of cold temperature constraints to productivity and a relative increase in other environmental controls such as moisture limitations (e.g. Kim et al. 2014a).

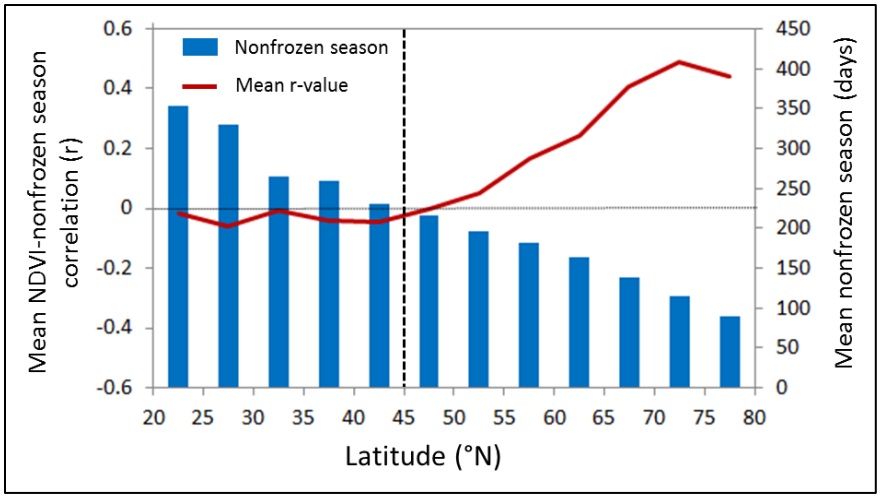

Figure 3. Latitudinal variation in mean correlations (r) between annual non-frozen season variations and summer (JJA) NDVI growth anomalies defined over a 9-year record (2000-2008) (after Kim et al. 2012, Fig 5b).

2.2 L3_FT_P PRODUCTION

An overview of the L3_FT_P processing sequence is provided in Figure 2. Research using SSM/I radiometer and SeaWinds-on-QuikSCAT scatterometer data indicate substantial variability of freeze/thaw spatial and temporal dynamics derived from AM and PM overpass data with important linkages to surface energy balance and carbon cycle dynamics (McDonald and Kimball, 2005; Kim et al., 2011). L3_FT_P algorithm products generated utilizing both ascending (PM) and descending (AM) radiometer data streams will enable regional assessment and monitoring of diurnal variability in terrestrial freeze/thaw state dynamics.

The L3_FT_P algorithm is applied to L1C_TB granules for unmasked land regions. The resulting intermediate freeze/thaw products (Figure 2) serve two purposes: (1) these data are assembled into global daily composites in production of the L3_FT_P product, and (2) the freeze/thaw product derived from global AM L1C_TB granules provide the binary freeze/thaw state flag supporting generation of the L2 and L3 soil moisture passive products.

The L3_FT_P algorithm is applied to the brightness temperature normalized polarization ratio (NPR). Decreases and increases in NPR are associated with landscape freezing and thawing transitions, respectively. The decrease in NPR under frozen conditions is a result of small increases in the V-pol brightness temperature combined with larger increases at H-pol (Rautiainen et al., 2012; 2014). Various studies have shown the NPR to be preferred over other approaches as it minimizes sensitivity to physical temperature and outperforms other L-band brightness temperature based approaches (Rautiainen et al., 2014; Roy et al., 2015).

L3_FT_P data processing will not occur over masked areas. It is anticipated that “no-data” flags will be associated with the L3_FT_P product identifying each of the masked surface types: ocean and inland open water (static open water fraction from MODIS), permanent ice and snow, and urban areas. The L3_FT_P algorithms utilize ancillary data during execution and processing

as summarized in Section 4.2.2. Ancillary data are also required to optimize the state change thresholds in the baseline algorithm scheme (see section 4.2.3).

2.3 Data Product Characteristics

The L3_FT_P product delineates freeze/thaw state on a pixel-wise basis according to the nomenclature in Table 4. An example binary FT image derived from SMAP radiometer measurements is shown in Figure 4.

Table 3. Nomenclature of the SMAP L3_FT_P product, indicating the landscape state as observed during AM and PM overpasses, and the corresponding freeze/thaw classification terminology.

Landscape State		**F/T Classification Terminology combining AM and PM data**
AM Overpass	**PM Overpass**	
Frozen	Frozen	Frozen
Thawed	Thawed	Thawed
Frozen	Thawed	Transitional
Thawed	Frozen	Inverse-Transitional

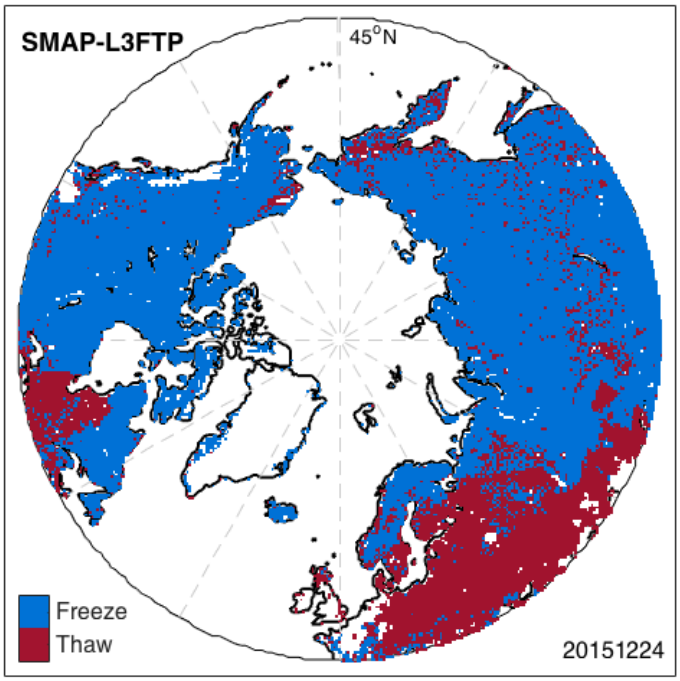

Figure 4. Binary freeze/thaw retrievals from SMAP radiometer measurements for 24 December 2015.

The L3_FT_P algorithm is applied to regridded L1C_TB radiometer data as a baseline (Figure 2). Implementing the L3_FT_P algorithm in this way ensures production of the binary state freeze/thaw flag consistent with the needs of L2/L3 soil moisture processing. The intermediate orbit-specific freeze/thaw products are temporally composited to assemble

freeze/thaw state maps separately for AM and PM acquisitions. The daily temporal compositing process is performed on the 36 km EASE grid data, retaining the freeze/thaw state associated with those acquisitions closest to 6:00 AM local time (AM daily product) and 6:00 PM local time (PM daily product). These intermediate products are further composited into the daily L3_FT_P product, keeping the latest date of acquisition as a replacement for acquisitions acquired on older dates, to ensure full coverage of the freeze/thaw domain from AM and PM acquisitions separately. These AM and PM multi-date composites are used to derive the combined product with nomenclature shown in Table 3 above. The respective date and time of acquisition of each of the AM and PM components of the data stream is maintained in the data set. The daily L3_FT_P product will thus incorporate AM and PM data for the current day, as well as past days' information (to a maximum of 3 days, necessary only near the southern margin of the FT domain) to ensure complete coverage of the freeze/thaw domain in each daily product.

Formatting of the L3_FT_P product is HDF5 with appropriate metadata. The L3_FT_P is posted to a polar grid - the projections are defined in terms of north polar azimuthal and global cylindrical Equal-Area Scalable Earth (EASE; version 2) grids (Armstrong and Brodzik, 1995). These gridding schemes are similar to current versions of the SSM/I derived FT ESDR (http://nsidc.org/data/NSIDC-0477).

Latency is defined as the average time under normal operating conditions between data acquisition by the SMAP observatory and delivery of the product to the data center. Latency of the baseline L3_FT_P product is dependent on the delivery rate of L1C_TB (135 MB per day) data from the radiometer processing system and on the rate at which these can be processed into freeze/thaw products and submitted to the SMAP NSIDC DAAC. Processing of the baseline L3_FT_P product will be complete within 24 hours of receipt of the global L1C_TB data, which itself has a latency of 12 hours.

3 PHYSICS OF THE PROBLEM

3.1 SYSTEM MODEL

The ability of microwave remote sensing instruments to observe freezing and thawing of a landscape has its origin in the distinct changes of surface dielectric properties that occur as water transitions between solid and liquid phases. A material's permittivity describes how that material responds in the presence of an electromagnetic field (Kraszewski, 1996). As an electromagnetic field interacts with a dielectric material, the resulting displacement of charged particles from their equilibrium positions gives rise to induced dipoles that respond to the applied field. A material's permittivity is a complex quantity (*i.e.*, having both real [ε'] and imaginary [ε''] numerical components) expressed as:

$$\varepsilon = \varepsilon' - j\varepsilon'' \tag{1}$$

and is often normalized to the permittivity of a vacuum (ε_0) and referred to as the relative permittivity, or the *complex dielectric constant*:

$$\varepsilon_r = \varepsilon'/\varepsilon_0 - j\varepsilon''/\varepsilon_0 = \varepsilon_r' - j\varepsilon_r''. \tag{2}$$

The real component of the dielectric constant, ε_r', is related to a material's ability to store electric field energy. The imaginary component of the dielectric constant, ε_r'', is related to the dissipation or energy loss within the material. At microwave wavelengths, the dominant phenomenon contributing to ε_r'' is the polarization of molecules arising from their orientation with the applied field. The dissipation factor, or *loss tangent*, is defined as the ratio:

$$\tan(\delta) = \varepsilon_r''/\varepsilon_r'. \quad (3)$$

Consisting of highly polar molecules, liquid water exhibits a dielectric constant that dominates the microwave dielectric response of natural landscapes (Ulaby *et al*., 1986). As liquid water freezes, the molecules become bound in a crystalline lattice, impeding the free rotation of the polar molecules and reducing the dielectric constant substantially. In general, landscapes of the terrestrial cryosphere consist of a soil substrate that may be covered by some combination of vegetation and seasonal or permanent snow. The sensitivity of radar and brightness temperature signatures to these landscape features is affected strongly by the sensing wavelength, as well as landscape structure and moisture conditions. The composite remote sensing signature represents a sampling of the aggregate landscape dielectric and structural characteristics, with sensor wavelength having a strong influence on the sensitivity of the remotely sensed signature to the various landscape constituents.

3.2 L-BAND BRIGHTNESS TEMPERATURE SENSITIVITY TO LANDSCAPE FREEZE/THAW

Microwave measurements at L-band can provide landscape freeze/thaw state information because of sensitivity to surface permittivity, which is predominantly influenced by the phase of water. As described in greater detail in Section 3.1, the presence of free liquid water in soils causes a high effective permittivity, while freezing of free liquid water in soils decreases the effective soil permittivity, and thus increases emissivity and brightness temperatures significantly. Temporal changes in the L-band brightness temperature are therefore related to the freezing or thawing of the surface, which can be exploited to retrieve the landscape freeze/thaw state (Rautiainen et al., 2016; Roy et al., 2015). The ratio of TBH (horizontal polarization) over TBV (vertical polarization) drastically increases during surface freeze, and remains high throughout the winter season (Brucker et al., 2014).

Compared to freeze/thaw products based on microwave sensors operating at higher frequencies (e.g. Kim et al., 2011), L-band observations exhibit deeper soil penetration depths, reduced influence from overlying vegetation, and hence increased sensitivity to the land surface freezing process (Rautiainen et al., 2014). While freeze/thaw transitions induce rapid changes in L-band brightness temperature, variables such as snow wetness, vegetation phenology, and soil moisture can complicate retrieval algorithm performance by imposing significant within and between season variability on the brightness temperature time series.

4 RETRIEVAL ALGORITHM

4.1 THEORETICAL DESCRIPTION

Derivation of the SMAP L3_FT_P product is based on a temporal change detection approach that has been previously developed and successfully applied using time-series satellite remote sensing radar backscatter and radiometric brightness temperature data from a variety of sensors at different spectral wavelengths and a range of spatial resolutions. The approach is to identify the landscape freeze/thaw via the temporal response of the normalized polarization ratio (NPR) of the brightness temperature to changes in the dielectric constant of the landscape components that occur as the water within the components transitions between frozen and non-frozen conditions. Classification algorithms assume that the large changes in dielectric constant occurring between frozen and non-frozen conditions dominate the corresponding NPR temporal dynamics across the seasons, rather than other potential sources of temporal variability such as changes in canopy structure and biomass or large precipitation events.

4.1.1 BASELINE ALGORITHM: SEASONAL THRESHOLD APPROACH

The SMAP L3_FT_P freeze/thaw algorithm is based on a seasonal threshold approach. While other freeze/thaw algorithmic approaches are possible (for example, moving window; temporal edge detection) these techniques do not fulfill the SMAP data latency requirement, and so are not discussed further in this document.

The seasonal threshold (baseline) algorithm examines the time series progression of the remote sensing signature relative to signatures acquired during seasonal reference frozen and thawed states. The algorithm is applied to the normalized polarization ratio (NPR) of SMAP radiometer measurements:

$$NPR = \frac{TBV - TBH}{TBV + TBH} \tag{4}$$

A seasonal scale factor Δ(t) is defined for an observation acquired at time *t* as:

$$\Delta t = \frac{NPR(t) - NPR(fr)}{NPR(th) - NPR(fr)} \tag{5}$$

where NPR(*t*) is the normalized polarization ratio calculated at time *t*, for which a freeze/thaw classification is sought, and NPR(th) and NPR(fr) are normalized polarization ratios corresponding to the frozen and thawed reference states, respectively. A major component of the SMAP baseline algorithm development involved application of existing satellite L-band measurements from the Aquarius mission over the FT domain to develop pre-launch maps of NPR_{th} and NPR_{fr}. These initial references were utilized for pre-launch preparatory activities, and were updated through post-launch integration of SMAP measurements (Section 4.2.3).

A threshold level *T* is then defined such that:

$$\begin{aligned} \Delta(t) &> T \\ \Delta(t) &\leq T \end{aligned} \tag{6}$$

defines the thawed and frozen landscape states, respectively. This series of equations (4-6) are run on a grid cell-by-cell basis for unmasked portions of the FT domain. The output from

Equation (6) is a dimensionless binary state variable designating either frozen or thawed conditions for each unmasked grid cell. The parameter *T* will be fixed at 0.5 across the entire FT domain at the start of the SMAP mission, but will be optimized after the freeze and thaw references are updated from the pre-launch Aquarius derived values to actual SMAP references (see Section. 4.2.3).

Following the pixel wise determination of freeze/thaw state, two additional processing steps are applied to mitigate summer season false freeze and winter season false thaw retrievals. First, if the brightness temperature magnitude at either V or H pol is greater than 273, the pixel is set to thaw regardless of the retrieval. Second, 'never frozen' and 'never thawed' masks (Figure 5) were calculated from daily AMSR-E and AMSR2 derived freeze/thaw maps (using the approach described in Kim et al., 2012) over the 2002-2015 period. These masks are then applied using a 31-day moving window approach to fix the retrieval state each day for pixels that never changed freeze/thaw state during the AMSR record:

$$NeverFrozen(doy) = \sum_{i=doy-15}^{doy+15} Freeze\_AMSR\_flag(i)$$
$$NF\_mask = (NF == 0) \quad (7)$$

$$NeverThawed(doy) = \sum_{i=doy-15}^{doy+15} Thaw\_AMSR\_flag(i)$$
$$NT\_mask = (NT == 0) \quad (8)$$

While these additional processing steps do not remove all false flags, they substantially reduce obviously false flags without relying on ancillary surface temperature information.

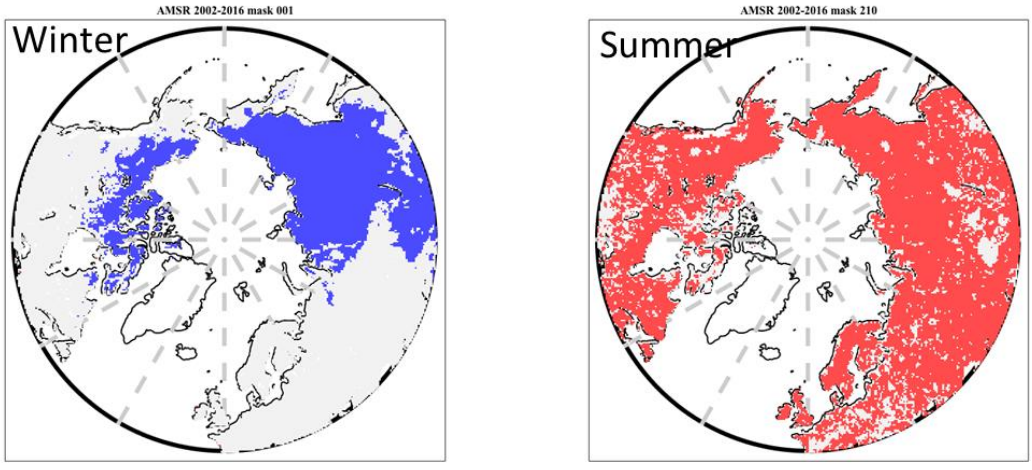

Figure 5. Example never thawed (left) and never frozen (right) masks for 1 January and 29 July.

4.2 PRACTICAL CONSIDERATIONS

4.2.1 ANCILLARY DATA AVAILABILITY/CONTINUITY

Ancillary datasets are used to (1) support initialization of the references and updating of the thresholds employed in the algorithm, (2) set flags that indicate potential problem regions, and (3) define masks where no retrievals should be performed. Ancillary datasets of inland open water, permanent ice and snow, and urban areas are used to derive masks so that no retrievals occur over these regions. Ancillary datasets of mountainous areas, fractional open water cover, and precipitation are used to derive flags so that a confidence interval can be associated with the retrieval. A primary source for each of the above ancillary parameters was selected. These data are common to all algorithms using that specific parameter. All ancillary datasets are resampled to a spatial scale and geographic projection that matches the L3_FT_P and L3_FT_P_E products in accordance with the guidelines of the SMAP ADT/SDT/ST. These data will be archived in a shared master file of ancillary data to ensure consistency across the SMAP data processing and algorithm product array.

Ancillary datasets used for L3_FT_P data processing were in place prior to launch, with no need for periodic updates during post-launch operations. A continuous surface map of fractional area of open water was used to represent fractional water coverage within a grid consistent with the resolution and projection of the L3_FT_P and L3_FT_P_E products. No further freeze/thaw data processing will occur for grid cells within masked regions. For the L3_FT_P and L3_FT_P_E development, the lake fraction threshold within a grid cell was set to 50%. Determination of a physically-based lake fraction will be finalized for the validated L3_FT_P release. Table 4 lists the ancillary data to be employed in support of L3_FT_P and L3_FT_P_E production. Similar ancillary data were used for production of the SMAP radar L3_FT_A product. Ancillary data sets are described in separate documents for each data set.

Table 4. Input datasets needed for generation of L3_FT_P

Data Type	Data Source	Frequency	Resolution	Extent	Use
Vegetation type	MODIS-IGBP	Once	250 m	Global	Sensitivity Analysis
Precipitation	ECMWF forecasts	Time of acquisition	0.25 degrees	Global	Sensitivity Analysis
Static Water bodies	MODIS44W	Once	250 m	Global	Mask/Flag
Mountainous Areas	NASA Global DEM	Once	30 m	Global	Mask/Flag
Permanent Ice and Snow	MODIS-IGBP permanent ice and snow class	Once	500 m	Global	Mask/Flag
Seasonal Snow	NOAA IMS	Daily	1 km	Northern Hemisphere	Flag
Never thawed/never frozen masks	AMSR-E; AMSR2	Daily	25 km	Northern Hemisphere	False flag mitigation

4.2.2 UPDATING AND OPTIMIZATION OF REFERENCES AND THRESHOLDS

Various techniques were tested pre-launch using Aquarius data for isolating measurements characteristic of frozen and thawed conditions, including temporal averages (i.e. during January/February for freeze; July/August for thaw) and averages of a fixed number of lowest/highest seasonal backscatter values. These pre-launch references (*NPR(th)*) were replaced with SMAP radiometer measurements from July and August 2015 (thaw) and January and February 2016 (freeze) for the northern (≥45°N) domain. The 20 highest (lowest) NPR values from these periods were retained and averaged to create the thaw (freeze) reference. Data were separated by ascending and descending orbit. Because of differences in the seasonal evolution of L-band brightness temperature compared to radar, which has generally greater temporal variability and sensitivity to parameters such as soil moisture and vegetation phenology, the methodological approach to NPR freeze and thaw references will be refined in future product releases. In addition, the reference values will be updated following each transition season. The initial SMAP freeze and thaw NPR references are shown in Figure 6.

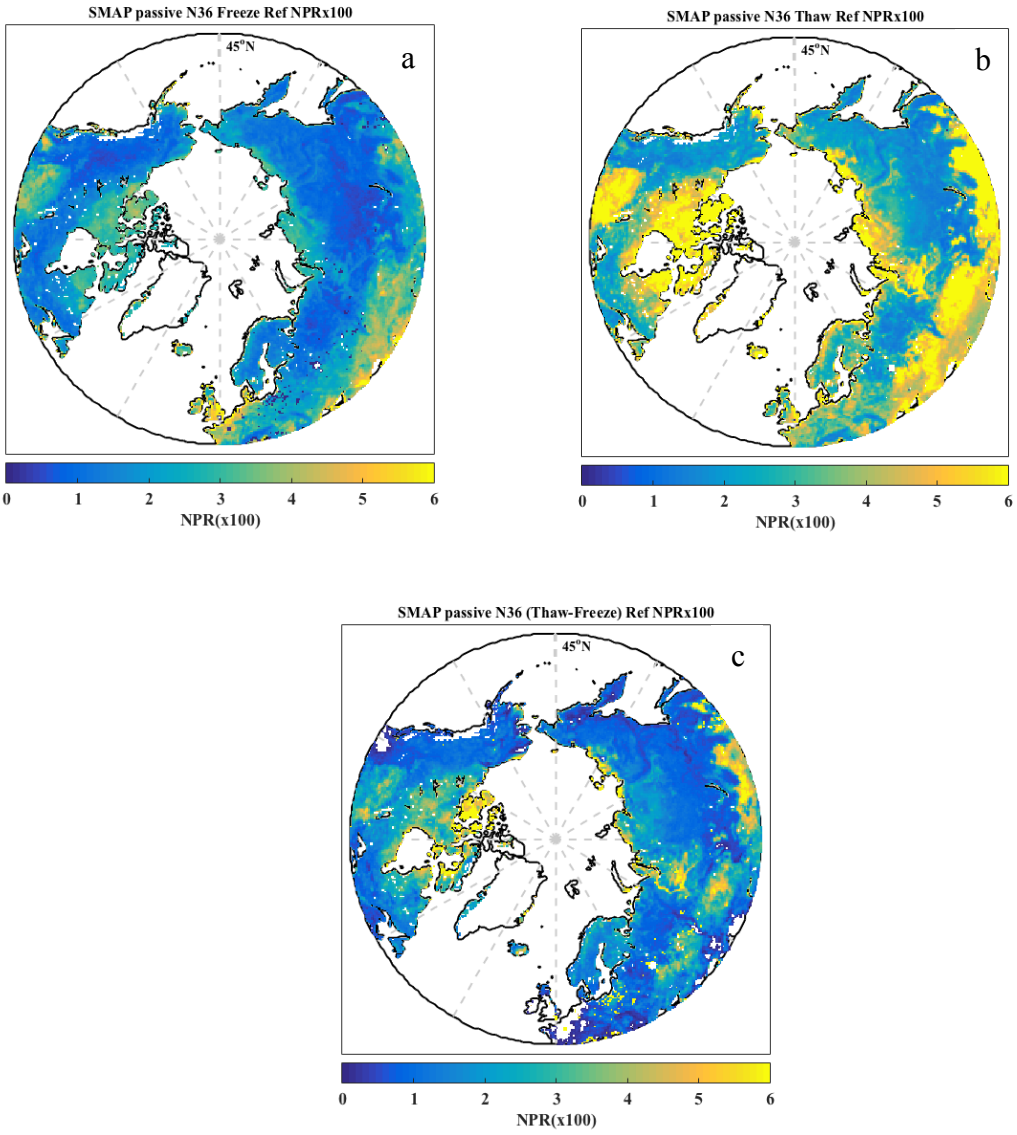

Figure 6. SMAP radiometer (a) freeze and (b) thaw references; (c) reference difference between panels (a) and (b). Units are NPR scaled by 100.

The freeze/thaw retrieval threshold (*T*) is fixed at 0.5. Pre-launch threshold (*T*) optimization experiments were conducted using Aquarius data and reanalysis derived estimates of air and surface soil temperature. Unique optimized thresholds were determined for ascending and descending overpasses, and freeze-to-thaw and thaw-to-freeze transitions, by applying a linear fit to values of Δt ($0.1 < \Delta t < 0.9$; see equation 5). The value of Δt at the intersect of temperature = 0 represents the optimized threshold. Optimization approaches will be evaluated using in situ measurements from the cal/val network in advance of future product releases.

4.2.3 CALIBRATION AND VALIDATION

The accuracy of the L3_FT_P products will be determined by comparison of the SMAP freeze/thaw retrievals with in situ measurements from sites within northern latitude (≥45°N) land areas. The same methodologies will be applied to both 36 and 9 km resolutions in order to determine any fundamental algorithm performance differences. The in situ validation data will include all core validation sites (Figure 7), and selected sites from sparse networks using criteria based on site representativeness (uniform and representative terrain and land cover.

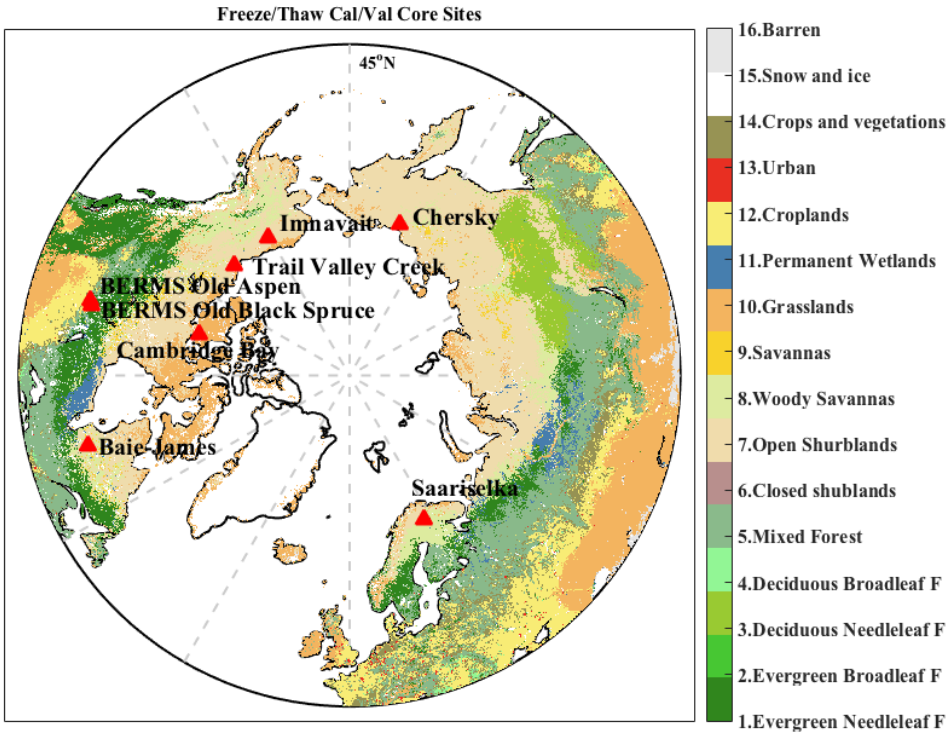

Figure 7. Freeze/thaw product cal/val sites.

The methodology is based on reference freeze/thaw flags derived from co-located air and soil temperature corresponding to the local time of the descending and ascending satellite overpasses. The computation of the classification accuracy proceeds as follows: Let $s_{AM/PM}(i,t) = 1$ if the L3_FT_P product at grid cell i (on the SMAP 36 km EASE grid) and time t indicates frozen conditions for AM (descending) or PM (ascending) overpass, respectively, and let $s_{AM/PM}(i,t) = 0$ if the L3_FT_P product indicates thawed conditions for AM or PM overpass, respectively. Likewise, let $v_{AM/PM}(i,t) = 1$ if the corresponding reference flag indicates frozen conditions at the AM or PM overpass, and $v(i,t) = 0$ for thawed conditions at the AM or PM overpass. Next, the error flag δ is set by comparing the SMAP product to the validating observations:

$$\delta_{AM/PM}(i,t) = \begin{cases} 0 & if\ s_{AM/PM}(i,t) = v_{AM/PM}(i,t) \\ 1 & if\ s_{AM/PM}(i,t) \neq v_{AM/PM}(i,t) \end{cases} \quad (9)$$

Note that a single L3_FT_P flag is produced each day, but is derived from separate descending (AM) and ascending (PM) overpasses. The L3_FT_P flags will therefore be separated back into binary freeze/thaw classes for the AM and PM orbits, producing two retrieval match-ups each day.

The mission Level 1 requirement will be satisfied if (for both AM and PM overpasses together):

$$1 - \left(\sum_{i=1}^{N_i} \sum_{t=1}^{N_t(i)} d(i,t) \right) \Big/ \left(\sum_{i=1}^{N_i} N_t(i) \right) \geq 0.8 \quad (10)$$

Equation 10 will be solved daily, to provide instantaneous determinations of freeze/thaw spatial accuracy, using the available reference sites. The mission requirement of 80% spatial accuracy will be assessed cumulatively (in a running manner with each new day of data added to the previous days). Assessment with the full suite of reference FT flags will allow algorithm performance metrics to be computed for various surface conditions (i.e. wet snow versus dry snow), and assist in determining the landscape components driving the radiometer response. Retrieval performance will also be summarized monthly to reduce sensitivity to prolonged periods of consistent frozen and thawed states in the winter and summer, respectively.

Daily comparison of the L3_FT_P freeze/thaw fields will therefore also be conducted with the modeled Tsurf output (mean of skin temperature and 10 cm soil temperature), and a FT product derived from SMOS L-band radiometer measurements (Rautiainen et al., 2014). These results will not be used to formally assess the FT mission requirement, but will be used as supplemental information to expand the temporal and spatial domain of the validation, and for evaluation of the freeze/thaw reference states and optimized thresholds. The comparisons to supplemental information are expected to reveal potential inconsistencies in the product performance on the global scale not identifiable with point observations.

Below 45°N, the AM overpass radar freeze/thaw retrievals, implemented as a "frozen soil" flag in the L3_SM_P product, will be evaluated as part of the L4_C cal/val activities, primarily through pixel-point assessments with WMO daily air temperature measurements.

4.2.4 Algorithm Baseline Selection

The current baseline algorithm is the algorithm of choice as it is best suited to fulfill mission requirements and facilitated the unplanned transition from SMAP radar to radiometer input. It is anticipated that research projects will examine additional radiometer freeze/thaw retrieval options, including single channel approaches and additional combinations of the brightness temperature measurements (e.g. Rautiainen et al 2014), the use of diurnal information, and the

application of algorithms to estimates of emissivity rather than brightness temperature. Further algorithm refinements may include the use of additional ancillary information for identifying and screening false freeze/thaw retrievals, or imposing additional quality flags.

5 CONSTRAINTS, LIMITATIONS, AND ASSUMPTIONS

Constraints and limitations of the algorithm will be assessed using the validation procedures described above (e.g. Section 4.2.4). The landscape freeze/thaw state retrieval represented by the L3_FT_P algorithm and products characterizes the predominant frozen or non-frozen state of the land surface within the sensor field-of-view (FOV) and does not distinguish freeze/thaw characteristics among different landscape elements, including surface snow, soil, open water or vegetation. The lower frequency L-band retrievals from SMAP are expected to have greater sensitivity to surface soil freeze/thaw conditions under low to moderate vegetation cover. Microwave freeze/thaw sensitivity is strongly constrained by intervening vegetation biomass, soil moisture levels, and snow wetness. Ambiguity in relating changes in the radiometer signal to these specific landscape components is a challenge to validation of the freeze/thaw product (Colliander et al., 2012). In northern, boreal and tundra landscapes L-band penetration depth and soil sensitivity is greater under frozen conditions when land surface liquid water levels are low, and markedly reduced under thawed conditions due to characteristically moist surface organic layer and soil active layer conditions, even under relatively low tundra vegetation biomass levels (Du et al. 2014).

The SMAP seasonal threshold freeze/thaw classification algorithm requires the establishment of accurate and stable frozen and non-frozen reference state conditions for each 36 km resolution grid cell. These references will be updated after each summer and winter seasons with new SMAP measurements. Reprocessing of the SMAP data record incorporating annual variations in the SMAP freeze/thaw reference states may improve product accuracy over the use of static reference conditions.

The resulting spatial classification error is expected to be larger at lower latitudes (i.e. <45°N) where freeze/thaw is ephemeral and the difference between frozen and thawed radar references is relatively small, and over complex terrain where freeze/thaw heterogeneity is larger. The freeze/thaw classification error may also be larger over densely vegetated areas due to vegetation scattering effects on microwave emissivity, which reduces Tb V and H-polarization differences and NPR dynamic range. In arid regions, the small amount water present in the thawed state makes the soil permittivity close to the frozen state, which can cause false freeze retrieval errors.

The SMAP L-band radiometer freeze/thaw retrievals are mapped at 36 km and 9 km resolution grids. The resulting freeze/thaw retrievals characterize the predominant frozen or non-frozen condition of the landscape within a grid cell and does not distinguish sub-grid scale freeze/thaw heterogeneity within the sensor FOV. Previous studies using finer resolution (~100m) satellite L-band SAR (JERS-1 and PALSAR) data over Alaska indicate that freeze/thaw classification error from sub-grid scale heterogeneity is greater over complex terrain and during seasonal freeze/thaw transitions; spatial classification error decreases as the sensor footprint

approaches the scale of landscape microclimate heterogeneity (Du et al. 2014, Podest et al. 2014).

A major assumption of the seasonal threshold based temporal change freeze/thaw classification is that the major temporal shifts in brightness temperature are caused by land surface dielectric changes from temporal freeze/thaw transitions. This assumption generally holds for higher latitudes and elevations where seasonal frozen temperatures are a significant part of the annual cycle and a large constraint to land surface water mobility and ecosystem processes (e.g., Kim et al. 2012). However, freeze/thaw classification accuracy is expected to be reduced where other environmental factors may cause large temporal shifts in brightness temperature, including large rainfall events and surface inundation, and changes in vegetation biomass (e.g. phenology, disturbance and land cover change). While there is a strong NPR response to freeze/thaw transitions, NPR is not stable during summer due to the influence of vegetation, soil moisture, etc. Depolarization of summer season measurements leads to false freeze retrievals that must be mitigated. Winter season false thaw in areas of complex terrain due to uncertainty in the references due to sub-grid heterogeneity.

The SMAP L3_FT_P product distinguishes 4 levels of freeze/thaw conditions determined from the ascending (6AM) and descending (6PM) orbit retrievals, including frozen (from both AM and PM overpass times), non-frozen (AM and PM), transitional (AM frozen; PM non-frozen) and inverse-transitional (AM non-frozen; PM frozen) states. The L3_FT_P product has sufficient fidelity and accuracy to distinguish diurnal freeze/thaw state changes common during seasonal transitions and temperate climate zones, and including frost-related impacts to vegetation productivity (e.g. Kim et al. 2014b).

6 REFERENCES

Armstrong, R.L. and M. J. Brodzik. (1995) An Earth-gridded SSM/I data set for cryospheric studies and global change monitoring. *Advances in Space Research*, **16(10)**, 155-163.

Betts, A. K., P. Viterbo, A. Beljaars, and B. van den Hurk. (2000) Impact of BOREAS on the ECMWF forecast model, *Journal of Geophysical Research*, **106(D24)**, 33,593-33,604.

Black, T. A., W. Chen, A. Barr, A. Arain, Z. Chen, Z. Nesic, E. Hogg, H. Neumann, and P. Yang. (2000) Increased carbon sequestration by a boreal deciduous forest in years with a warm spring. *Geophysical Research Letters*, **27(9)**, 1271-1274.

Brucker, L., E. Dinnat, and L. S. Koenig. (2014). Weekly gridded Aquarius L-band radiometer/scatterometer observations and salinity retrievals over the polar regions—Part 2: Initial product analysis. *Cryosphere*, **8**, 915–930.

Churkina, G., and S. Running. (1998) Contrasting climatic controls on the estimated productivity of different biomes. *Ecosystems*, **1**, 206-215.

Colliander, A., K. McDonald, R. Zimmermann, R Schroeder, J. Kimball, and E Njoku. (2012) Application of QuikSCAT Backscatter to SMAP Validation Planning: Freeze/Thaw State Over ALECTRA Sites in Alaska From 2000 to 2007. *IEEE Transactions on Geoscience and Remote Sensing*, **50(2)**, 461-468.

Du, J., J. S. Kimball, M. Azarderakhsh, R.S. Dunbar, M. Moghaddam, and K.C. McDonald. (2014) Classification of Alaska spring thaw characteristics using satellite L-band Radar remote sensing. *Transactions in Geoscience and Remote Sensing*, DOI:10.1109/TGRS.2014.2325409.

Entekhabi, D., E. Njoku, P. Houser, M. Spencer, T. Doiron, J. Smith, R. Girard, S. Belair, W. Crow, T. Jackson, Y. Kerr, J. Kimball, R. Koster, K. McDonald, P. O'Neill, T. Pultz, S. Running, J.C. Shi, E. Wood, and J. Van Zyl. (2004) The Hydrosphere State (HYDROS) mission concept: An Earth System Pathfinder for global mapping of soil moisture and land freeze/thaw. *Transactions in Geoscience and Remote Sensing*, **42(10)**, 2184-2195.

Entekhabi, D., E. Njoku, P. O'Neill, K. Kellogg, W. Crow, W. Edelstein, J. Entin, S. Goodman, T. Jackson, J. Johnson, J. Kimball, J. Piepmeier, R. Koster, K. McDonald, M. Moghaddam, S. Moran, R. Reichle, J. C. Shi, M. Spencer, S. Thurman, L. Tsang, J. Van Zyl. (2010) The Soil Moisture Active and Passive (SMAP) Mission. *Proceedings of the IEEE*, **98(5).**

Frolking S., K. McDonald, J. Kimball, R. Zimmermann, J.B. Way and S.W. Running. (1999). Using the space-borne NASA Scatterometer (NSCAT) to determine the frozen and thawed seasons of a boreal landscape. *Journal of Geophysical Research*, **104(D22)**, 27,895-27,907.

Gamon, J.A., K.F. Huemmrich, J. Chen, D. Fuentes, F.G. Hall, J.S. Kimball, S. Goetz, J. Gu, K.C. McDonald, J.R. Miller, M. Moghaddam, D.R. Peddle, A.F. Rahman, J.-L. Roujean, E.A. Smith, C.L. Walthall, and P. Zarco-Tejada. (2004) Remote sensing in BOREAS: Lessons learned. *Remote Sensing of Environment*, **89(2)**, 139-162.

Goulden, M.L., S. Wofsy, J. Harden, S. Trumbore, P. Crill, S. Gower, T. Fries, B. Daube, S. Fan, D. Sutton, A. Bazzaz, and J. Munger. (1998) Sensitivity of boreal forest carbon balance to soil thaw. *Science* **279(9)**, 214-217.

Jarvis, P., and S. Linder. (2000) Constraints to growth of boreal forests. *Nature*, **405**, 904-905.

Kim, Y., J.S. Kimball, K. Zhang, K. Didan, I. Velicogna, and K.C. McDonald. (2014a) Attribution of divergent northern vegetation growth responses to lengthening non-frozen seasons using satellite optical-NIR and microwave remote sensing. *International Journal of Remote Sensing*, **35(10)**, 3700-3721.

Kim, Y., J. Kimball, K. Didan, and G. Henebry. (2014b) Response of vegetation growth and productivity to spring climateindicators in the conterminous United States derived from satelliteremote sensing data fusion. *Agriculture And Forest Meteorology*, **194**, 132–143.

Kim, Y., J.S. Kimball, K.C. McDonald and J. Glassy. (2011) Developing a global data record of daily landscape freeze/thaw status using satellite passive microwave remote sensing. *IEEE Transactions on Geoscience and Remote Sensing*, **49**, 949-960.

Kim, Y., J. Kimball, K. Zhang, and K. McDonald. (2012) Satellite detection of increasing Northern Hemisphere non-frozen seasons from 1979 to 2008: Implications for regional vegetation growth. *Remote Sensing of Environment*, **121**, 472–487.

Kimball, J., K. McDonald, A. Keyser, S. Frolking, and S. Running. (2001) Application of the NASA Scatterometer (NSCAT) for Classifying the Daily Frozen and Non-Frozen Landscape of Alaska, *Remote Sensing of Environment*, **75**, 113-126.

Kimball, J.S., K.C. McDonald, S.W. Running, and S. Frolking. (2004a). Satellite radar remote sensing of seasonal growing seasons for boreal and subalpine evergreen forests. *Remote Sensing of Environment*, **90**, 243-258.

Kimball, J.S., M. Zhao, K.C. McDonald, F.A. Heinsch, and S. Running. (2004b) Satellite observations of annual variability in terrestrial carbon cycles and seasonal growing seasons at high northern latitudes. In *Microwave Remote Sensing of the Atmosphere and Environment* IV, G. Skofronick Jackson and S. Uratsuka (Eds.), Proceedings of SPIE – The International Society for Optical Engineering, **5654**, 244-254.

Kraszewski, A. (editor) (1996) *Microwave Aquametry: Electromagnetic Wave Interaction with Water-Containing Materials*, IEEE Press, Piscataway, N.J., 484 pp.

Kuga, Y., M. Whitt, K. McDonald, F. and Ulaby. (1990) Scattering Models for Distributed Targets. In *Radar Polarimetry for Geoscience Applications*, Ulaby F. T. and Elachi C.,(Ed.), Artech House: Dedham, MA.

McDonald, K.C, and J.S. Kimball. (2005) Hydrological application of remote sensing: Freeze-thaw states using both active and passive microwave sensors. In *Encyclopedia of Hydrological Sciences*. Vol. 5., M.G. Anderson and J.J. McDonnell (Eds.), John Wiley & Sons Ltd.

McDonald, K.C., J.S. Kimball, E. Njoku, R. Zimmermann, and M. Zhao. (2004) Variability in springtime thaw in the terrestrial high latitudes: Monitoring a major control on the biospheric assimilation of atmospheric CO_2 with spaceborne microwave remote sensing. *Earth Interactions*, **8(20)**, 1-23.

National Research Council. (2007) *Earth Science and Applications from Space: National Imperatives for the Next Decade and Beyond*. pp. 400.

Nemani, R.R., C. Keeling, H. Hashimoto, W. Jolly, S. Piper, C. Tucker, R. Myneni, and S. Running. (2003) Climate-driven increases in global terrestrial net primary production from 1982 to 1999. *Science*, **300**, 1560-1563.

Podest, E. (2006), *Monitoring Boreal Landscape Freeze/Thaw Transitions with Spaceborne Microwave Remote Sensing*. Ph.D. dissertation, University of Dundee.

Podest, E., K.C. McDonald, and J.S. Kimball. (2014) Multi-sensor microwave sensitivity to freeze-thaw dynamics across a complex boreal landscape. *Transactions in Geoscience and Remote Sensing*, **52**, 6818-6828.

Raney, K. R. (1998), Radar fundamentals: Technical perspective, In *Principles and Applications of Imaging Radar*, Vol. 2, F. M. Henderson and A. J. Lewis (Eds.), John Wiley and Sons Inc., New York, pp. 9-130.

Rautiainen, K., J. Lemmetyinen, M. Schwank, A. Kontu, C. Ménard, C. Mätzler, M. Drusch, A. Wiesmann, J. Ikonen, and J. Pulliainen. (2014) Detection of soil freezing from L-band passive microwave observations, *Remote Sensing of Environment*, **147**, 206–218.

Rautiainen, K., T. Parkkinen, J. Lemmetyinen, M. Schwank, A. Wiesmann, J. Ikonen, C. Derksen, S. Davydov, A. Davydova, J. Boike, M. Langer, M. Drusch and J. Pulliainen. (2016) SMOS prototype algorithm for detecting autumn soil freezing, *Remote Sensing of Environment,* **180**, 346–360.

Rawlins, M.A, K.C. McDonald, S. Frolking, R.B. Lammers, M. Fahnestock, J.S. Kimball, C.J. Vorosmarty. (2005) Remote Sensing of Pan-Arctic Snowpack Thaw Using the SeaWinds Scatterometer, *Journal of Hydrology*, **312/1-4,** 294-311.

Rignot E., and Way, J.B. (1994) Monitoring freeze-thaw cycles along north-south Alaskan transects using ERS-1 SAR, *Remote Sensing of Environment*, **49**, 131-137.

Rignot, E., Way, J.B., McDonald, K., Viereck, L., Williams, C., Adams, P., Payne, C., Wood, W., and Shi, J. (1994) Monitoring of environmental conditions in taiga forests using ERS-1 SAR, *Remote Sensing of Environment*, ***49***, 145-154.

Roy, A., A. Royer, C. Derksen, L. Brucker, A. Langlois, A. Mialon and Y. Kerr. (2015) Evaluation of spaceborne L-band radiometer measurements for terrestrial freeze/thaw retrievals in Canada, *IEEE Journal of Selected Topics in Applied Earth Observations and Remote Sensing*, 10.1109/JSTARS.2015.2476358.

Ulaby, F. T., R. Moore, and A. Fung. (1986) *Microwave Remote Sensing: Active and Passive, Vol. 1-3*, Artec House: Dedham MA.

Ulaby, F. T., K. Sarabandi, K. McDonald, M. Whitt, and M. Dobson. (1990). Michigan Microwave Canopy Scattering Model (MIMICS), *International Journal of Remote Sensing*, **11(7),** 1223-1253.

Vaganov, E.A., M. Hughes, A. Kirdyanov, F. Schweingruber, and P. Silkin. (1999) Influence of snowfall and melt timing on tree growth in subarctic Eurasia. *Nature*, **400**, 149-151.

Way, J. B., J. Paris, E. Kasischke, C. Slaughter, L. Viereck, N. Christensen, M. Dobson, F. Ulaby, J. Richards, A. Milne, A. Sieber, F. Ahern, D. Simonett, R. Hoffer, M. Imhoff, and J. Weber. (1990) The

effect of changing environmental conditions on microwave signatures of forest ecosystems: preliminary results of the March 1988 Alaskan aircraft SAR experiment. *International Journal of Remote Sensing*, **11**, 1119-1144.

Way, J. B., R. Zimmermann, E. Rignot, K. McDonald, and R. Oren. (1997) Winter and Spring Thaw as Observed with Imaging Radar at BOREAS, *Journal of Geophysical Research,* **102(D24),** 29673-29684.

Wegmuller, U. (1990), The effect of freezing and thawing on the microwave signatures of bare soil, *Remote Sensing of Environment,* **33**, 123-135.

Wismann, V. (2000) Monitoring of seasonal thawing in Siberia with ERS scatterometer data. *IEEE Transactions on Geoscience and Remote Sensing*, **38**, 1804–1809.

Xu, X., C. Derksen, S. Yueh, R. S. Dunbar, and A. Colliander. (In press) Freeze/thaw detection and validation using Aquarius' L-band backscattering data, *IEEE Journal of Selected Topics in Applied Earth Observations and Remote Sensing.*

APPENDIX 1: GLOSSARY

[**Adapted from**: Earth Observing System Data and Information System (EOSDIS) Glossary http://www-v0ims.gsfc.nasa.gov/v0ims/DOCUMENTATION/GLOS-ACR/glossary.of.terms.html.]

ALGORITHM. (1) Software delivered by a science investigator to be used as the primary tool in the generation of science products. The term includes executable code, source code, job control scripts, as well as documentation. (2) A prescription for the calculation of a quantity; used to derive geophysical properties from observations and to facilitate calculation of state variables in models.

ANCILLARY DATA. Data other than instrument data required to perform an instrument's data processing. They include orbit data, attitude data, time information, spacecraft engineering data, calibration data, data quality information, data from other instruments (spaceborne, airborne, ground-based) and models.

BROWSE. A representation of a data set or data granule used to pre-screen data as an aid to selection prior to ordering. A data set, typically of limited size and resolution, created to rapidly provide an understanding of the type and quality of available full resolution data sets. It may also enable the selection of intervals for further processing or analysis of physical events. For example, a browse image might be a reduced resolution version of a single channel from a multi-channel instrument. Note: Full resolution data sets may be browsed.

BROWSE DATA PRODUCT. Subsets of a larger data set, generated for the purpose of allowing rapid interrogation (i.e., browse) of the larger data set by a potential user. For example, the browse product for an image data set with multiple spectral bands and moderate spatial resolution might be an image in two spectral channels, at a degraded spatial resolution. The form of browse data is generally unique for each type of data set and depends on the nature of the data and the criteria used for data selection within the relevant scientific disciplines.

Dynamic Browse. Refers to the generation of a browse product, including subsetting and/or resampling of data, by command of the user engaged in the browse activity. The browse data set is built in real-time, or near-real-time, as part of the browse activity.

Static Browse. Refers to interrogation of browse products which have been generated (through subsetting and/or resampling) before any user browses that particular data set.

CALIBRATION. (1) The activities involved in adjusting an instrument to be intrinsically accurate, either before or after launch (i.e., "instrument calibration"). (2) The process of collecting instrument characterization information (scale, offset, nonlinearity, operational, and environmental effects), using either laboratory standards, field standards, or modeling, which is used to interpret instrument measurements (i.e., "data calibration").

CALIBRATION DATA. The collection of data required to perform calibration of the instrument science and engineering data, and the spacecraft or platform engineering data. It includes pre-flight calibrator measurements, calibration equation coefficients derived from calibration software routines, and ground truth data that are to be used in the data calibration processing routine.

CORRELATIVE DATA. Scientific data from other sources used in the interpretation or validation of instrument data products, e.g. ground truth data and/or data products of other instruments. These data are not utilized for processing instrument data.

DATA PRODUCT. A collection (1 or more) of parameters packaged with associated ancillary and labeling data. Uniformly processed and formatted. Typically uniform temporal and spatial resolution. (Often the collection of data distributed by a data center or subsetted by a data center for distribution.) There are two types of data products:

Standard - A data product produced by a community consensus algorithm. Typically produced for a wide community. May be produced routinely or on-demand. If produced routinely, typically produced over most or all of the available independent variable space. If produced on-demand, produced only on request from users for particular research needs typically over a limited range of independent variable space.

Special - A data product produced by a research status algorithm. May migrate to a community consensus algorithm at a later time. If adequate community interest exists, the product may be archived and distributed by a DAAC.

DATA PRODUCT LEVEL. Data levels 1 through 4 as designated in the EOSDIS Product Type and Processing Level Definitions document.

Raw Data - Data in their original packets, as received from the observer, unprocessed.

Level 0 - Raw instrument data at original resolution, time ordered, with duplicate packets removed.

Level 1A - Reconstructed unprocessed instrument data at full resolution, time referenced, and annotated with ancillary information, including radiometric and geometric calibration coefficients and georeferencing parameters (i.e., platform ephemeris) computed and appended, but not applied to Level 0 data.

Level 1B - Radiometrically corrected and geolocated Level 1A data that have been processed to sensor units.

Level 1C - Level 1B data that have been spatially resampled.

Level 2 - Derived geophysical parameters at the same resolution and location as the Level 1 (1B or 1C) data.

Level 3 - Geophysical or sensor parameters that have been spatially and/or temporally re-sampled (i.e., derived from Level 2 or Level 1 data).

Level 4 - Model output and/or results of lower level data that are not directly derived by the instruments.

DISTRIBUTED ACTIVE ARCHIVE CENTER (DAAC). An EOSDIS facility that archives, and distributes data products, and related information. An EOSDIS DAAC is managed by an institution such as a NASA field center or a university, under terms of an agreement with NASA. Each DAAC contains functional elements for archiving and disseminating data, and for user services and information management. Other (non-NASA) agencies may share management and funding responsibilities for the active archives under terms of agreements negotiated with NASA.

GRANULE. The smallest aggregation of data which is independently managed (i.e., described, inventoried, retrievable). Granules may be managed as logical granules and/or physical granules.

GUIDE. A detailed description of a number of data sets and related entities, containing information suitable for making a determination of the nature of each data set and its potential usefulness for a specific application.

INSTRUMENT DATA. Data specifically associated with the instrument, either because they were generated by the instrument or included in data packets identified with that instrument. These data consist of instrument science and engineering data, and possible ancillary data.

Instrument Engineering Data. Data produced by the engineering sensor(s) of an instrument that is used to determine the physical state of an instrument in order to operate it, monitor its health, or aid in processing its science data.

Instrument Science Data. Data produced by the science sensor(s) containing the primary observables of an instrument, usually constituting the mission of that instrument.

METADATA. (1) Information about a data set which is provided by the data supplier or the generating algorithm and which provides a description of the content, format, and utility of the data set. Metadata provide criteria which may be used to select data for a particular scientific investigation. (2) Information describing a data set, including data user guide, descriptions of the data set in directories, and inventories, and any additional information required to define the relationships among these.

NEAR REAL-TIME DATA. Data from the source that are available for use within a time that is short in comparison to important time scales in the phenomena being studied.

ORBIT DATA. Data that represent spacecraft locations. Orbit (or ephemeris) data include: Geodetic latitude, longitude and height above an adopted reference ellipsoid (or distance from the center of mass of the Earth); a corresponding statement about the accuracy of the position and the corresponding time of the position (including the time system); some accuracy requirements may be hundreds of meters while other may be a few centimeters.

PARAMETER. A measurable or derived variable represented by the data (e.g. air temperature, snow depth, relative humidity.

QUICK-LOOK DATA. Data available for examination within a short time of receipt, where completeness of processing is sacrificed to achieve rapid availability.

RAW DATA. Numerical values representing the direct observations output by a measuring instrument transmitted as a bit stream in the order they were obtained. (Also see DATA PRODUCT LEVEL.)

REAL-TIME DATA. Data that are acquired and transmitted immediately to the ground (as opposed to playback data). Delay is limited to the actual time (propagation delays) required to transmit the data.

SPACECRAFT ENGINEERING DATA. Data produced by the engineering sensor(s) of a spacecraft that are used to determine the physical state of the spacecraft, in order to operate it or monitor its health.